



Nonclassical Properties of a Hybrid NAAN Quantum State

Gang Ren¹ · Hai-jun Yu¹ · Chun-zao Zhang¹ · Feng Chen²

Received: 24 February 2023 / Accepted: 27 March 2023 / Published online: 4 April 2023

© The Author(s), under exclusive licence to Springer Science+Business Media, LLC, part of Springer Nature 2023

Abstract

We introduce a two-mode hybrid entangled state (NAAN) which is constructed by two n -photon Fock states and two coherent states with an arbitrary relative phase. We show that the NAAN can be considered as the superpositions of NOON states when $\alpha \neq 0$. In the special case, when $\alpha = 0$, the NAAN degenerates to the general NOON. The most interesting nonclassical properties of this state are its strong violations of the CHSH inequality. In addition, we show explicitly some typical nonclassical properties of the NAAN state, such as entanglement, sub-Poissonian distribution, phase fluctuation and squeezing. These findings suggest that the even NAAN states exhibit a high degree of entanglement, while the odd NAAN states have a distinct sub-Poissonian distribution and the optimal phase sensitivity.

Keywords Hybrid entangled state · Phase estimation · Squeezing · CHSH inequality · Sub-Poissonian distribution

1 Introduction

In recent years, the generation of various nonclassical states and the study of their nonclassical characteristic have become the most fascinating aspects of quantum optics and quantum information [1–5]. The concepts of entangled states are related to interference of two different quantum states [6–8]. Entangled states have many applications for quantum information processing, such as quantum teleportation, quantum-key distribution, and dense coding [9–12]. Quantum technologies based on two photons entangled states can exhibit some interesting non-classical properties, such as nonlocality, entanglement, squeezing, the standard quantum limit of phase estimation [13–16].

Using several non-Gaussian operations, various types of entangled states have been produced, such as photon-added coherent states, photon-subtraction state [17, 18]. In addition, nonclassical states can also be generated by linear superposition of two standard coherent states with opposite phase, i.e., Schrödinger cat states [19, 20]. It has been reported that the even cat state exhibits the squeezing effect but has no antibunching effect, while the

✉ Gang Ren
renfeiyu@mail.ustc.edu.cn

¹ School of Electronic Engineering, Huainan Normal University, Huainan 232001, Anhui, China

² Institute of Advanced Manufacturing Engineering, Hefei University, Hefei 230022, China

odd cat state owns an antibunching effect but has no squeezing effect [21, 22]. It is worth noting that these non-classical quantum states are related to coherent states and belong to continuous-variable (CV) quantum states [23–25].

CV and discrete-variable (DV) quantum state are two major issues of quantum science. A typical DV entangled state is the NOON state $|\psi\rangle_{\text{NOON}} = (|N_1\rangle|0_2\rangle + |0_1\rangle|N_2\rangle)$, where N is the photon number and the subscript denotes the corresponding mode. Such states can be considered as macroscopic quantum superposition like cat states [26–30]. In quantum optics, the NOON states are considered as the heart of many quantum-enhanced measurement schemes, such as quantum lithography, quantum metrology [31, 32]. To date, five-photon NOON states have been prepared experimentally [33].

Recently, a type of hybrid entangled states (HES) in the combination of DV (a single photon number state) and CV (a coherent state) resources has been prepared in a free-travelling field [34–36]. Moreover, Kreis and van Loock have studied various kinds of HES between CV and DV. Many schemes for the generation of HES have been proposed by using hybrid quantum devices in atomic and molecular physics and quantum optics [37].

The aim of this paper is to construct a new hybrid quantum and to explore its several novel nonclassical properties. We begin by introducing the new state and deriving its normalization constant in Section 2. It will then go on to investigate its entanglement witnesses via degree of entanglement and Einstein–Podolsky–Rosen(EPR)criterion in Section 3. Section 4 will consider both the quantum statistical distribution and nonlocality by Mandel parameter, Wigner function and CHSH inequality. The purpose of the Section 5 is to analyze the phase sensitivity using parity detection and classical Fisher information. Section 6 seeks to find the squeezing properties with sum squeezing and difference squeezing. The final section gives a summary and main conclusion of the findings.

2 NAAN and its Normalization Constant

Let us start with a definition of bipartite NAAN as

$$|\psi\rangle = N_c^{-1/2}(|N_1\rangle|\alpha_2\rangle + e^{i\varphi}|\alpha_1\rangle|N_2\rangle), \quad (1)$$

where φ is a relative phase between $|N_1\rangle|\alpha_2\rangle$ and $|\alpha_1\rangle|N_2\rangle$, N_c is the normalization constant. The subscripts 1 and 2 will be used in this paper to refer to distinguish variables from different quantum light field modes. For the convenience of analysis, in the following discussion, we take

$$n \equiv n_1 = n_2, \quad \alpha \equiv \alpha_1 = \alpha_2, \quad (2)$$

where n_1, n_2 denote the average photon number in the mode 1 and 2.

According to the properties of quantum states $\text{Tr}\rho = 1$ and

$$\langle N_1 | \alpha_1 \rangle = \langle N_2 | \alpha_2 \rangle = \frac{\alpha^n}{\sqrt{n!}} e^{-\frac{1}{2}|\alpha|^2}, \quad (3)$$

the normalization constant is obtained as

$$N_c = 2 \left(\frac{1}{n!} |\alpha|^{2n} e^{-|\alpha|^2} \cos \varphi + 1 \right). \quad (4)$$

In particular, when $\varphi = \alpha = 0$, Eq. (1) reduces to the NOON state $|\psi\rangle_{Noon}$. However, when $N = 0$, $\alpha = 1$,

$$|\psi\rangle_{0110} = \frac{1}{\sqrt{2(1+e)}} \sum_{m=0}^{\infty} \frac{1}{m!} \left(a_2^{\dagger m} + e^{i\varphi} a_1^{\dagger m} \right) |0_1\rangle |0_2\rangle, \quad (5)$$

where we have used

$$|\alpha\rangle_{\alpha=1} = e^{-\frac{1}{2}+a^\dagger} |0\rangle = e^{-\frac{1}{2}} \sum_{m=0}^{\infty} \frac{a^{\dagger m}}{m!} |0\rangle. \quad (6)$$

Thus, it is easy to see that when $\varphi = 0, \pi$, the quantum states in Eq. (5) are different from the Bell states in Fock state [38, 39]

$$|\psi^\pm\rangle = \frac{1}{\sqrt{2}} (|01\rangle \pm |10\rangle). \quad (7)$$

To our knowledge, the NAAN state in Eq. (1) has not been previously studied and represents a novel symmetric HES which may be considered as a superposition of the NOON states..

3 Entanglement Witnesses

This section will examine the entanglement of the NAAN state via the von Neumann entropy of entanglement and EPR criterion.

3.1 Degree of Entanglement

Different methods have been used to measure the degree of entanglement via different kinds of entropies, such as entropy of entanglement and logarithmic negativity. For the two-mode entangled state, the von Neumann entropy of entanglement is defined as [40, 41]

$$E_v(\rho) = S[\text{Tr}_2(\rho)], \quad (8)$$

where $S[\rho] = -\text{Tr}(\rho \log_2 \rho)$ is von Neumann entropy, c_l and $\text{Tr}_2(\rho)$ denotes the partial transpose of density operator ρ with respect to 2-mode. For a two-mode pure state, its Schmidt decomposition is

$$|\psi_{12}\rangle = \sum_{k=0}^{\infty} c_k |\alpha_{k1}\rangle |\beta_{k2}\rangle, \quad (9)$$

where $|\alpha_{k1}\rangle$ and $|\beta_{k2}\rangle$ are orthogonal and normalized basis states and c_k are the superposition coefficients of the basis states [42, 43].

Substituting Eq. (9) into Eq. (8), the von Neumann entropy is obtained as

$$E_v(\rho) = - \sum_{k=0}^{\infty} |c_k|^2 \log_2 |c_k|^2. \quad (10)$$

Thus for the NAAN state shown in Eq. (1), in the number state basis one find that

$$|\psi\rangle = N_c^{-1/2} \sum_{m_1, m_2=0}^{\infty} |m_1\rangle |m_2\rangle \langle m_1 | (|N_1\rangle |\alpha_2\rangle + e^{i\varphi} |\alpha_1\rangle |N_2\rangle). \tag{11}$$

The von Neumann entropy for the NAAN can be obtained

$$E_v(\rho) = -|\omega|^2 \log_2 |\omega|^2, \tag{12}$$

where

$$\omega = N_c^{-1/2} \frac{1}{\sqrt{n!}} \alpha^n e^{-\frac{1}{2}|\alpha|^2} (1 + e^{i\varphi}). \tag{13}$$

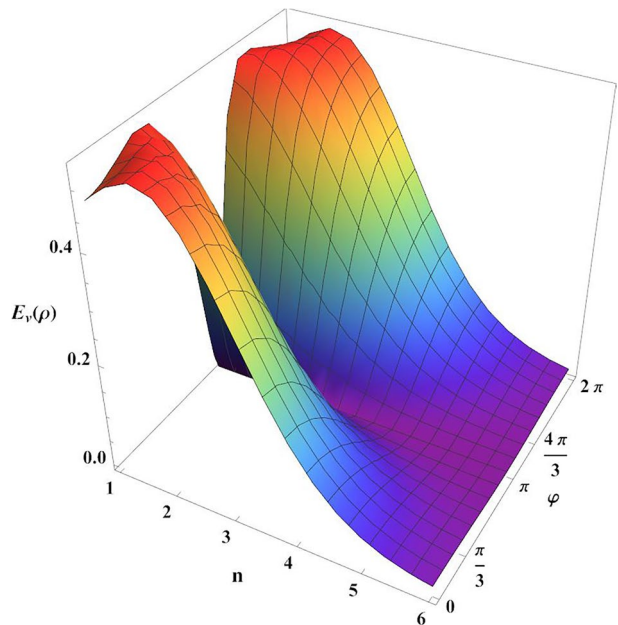
Here we should point out that when $n = 0, \alpha = 1, \varphi = 0, E_v(\rho) \rightarrow 0.5$, which is just the maximally entangled coherent states in Ref. [44]. When $\varphi = \pi$ and $n \neq 0, E_v(\rho) = 0$, which implies that the odd NAAN state has the lowest degree of entanglement.

For evaluating the degree of entanglement of the NAAN state, we plot the von Neumann entropy of entanglement for the NAAN states as a function of both n and φ via Eq. (12). One obvious conclusion is that the degree of entanglement decreases rapidly as the value of n increases. In addition, when n is fixed, the entanglement degree of NAAN states is distributed symmetrically about $\varphi = \pi$. The even NAAN states ($\varphi = 0, 2\pi$) have a high degree of entanglement (Fig. 1).

3.2 EPR Criterion

EPR criterion is used to investigate an inseparability of the two-mode state via a pair of EPR-type operators [45, 46]

Fig. 1 The von Neumann entropy of entanglement for the NAAN states as a function of both n and φ in the case of $\alpha = 1$. The value of n ranges from 1 to 6 and that of φ ranges from 0 to 2π .



$$EPR = \Delta^2(X_1 - X_2) + \Delta^2(P_1 + P_2), \tag{14}$$

where $X_k = (a_k + a_k^\dagger)/\sqrt{2}$ and $P_k = (a_k - a_k^\dagger)/\sqrt{2}i$ ($k = 1, 2$).

Using $\Delta^2 O = \langle O^2 \rangle - \langle O \rangle^2$, we get

$$EPR = 2 \left[\langle a_1^\dagger a_1 + a_2^\dagger a_2 \rangle - 2 \langle a_1 a_2 + a_1^\dagger a_2^\dagger \rangle - [Re \langle a_1 - a_2 \rangle]^2 - [Im \langle a_1 + a_2 \rangle]^2 + 1 \right]. \tag{15}$$

In principle, the EPR criterion of arbitrary inseparable two-mode states satisfies the condition of $EPR < 2$. To obtain EPR for the NAAN state, we need to calculate the average values of $a_1^\dagger a_1, a_1 a_2$ and a_1 as (see Appendix 1)

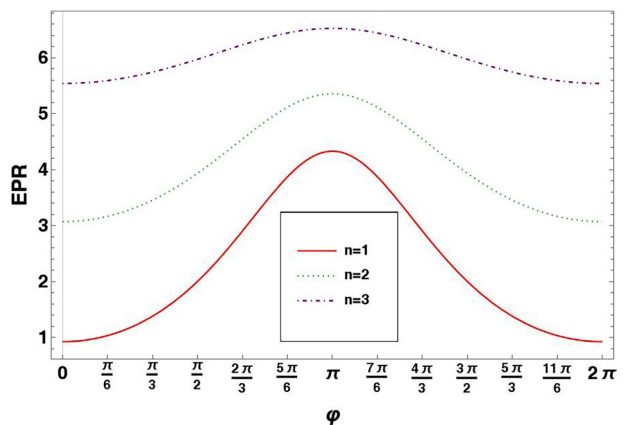
$$\begin{aligned} E_1 &\equiv \langle a_1^\dagger a_1 \rangle = \langle a_2^\dagger a_2 \rangle \\ &= N_c^{-1} \left(\frac{2}{(n-1)!} |\alpha|^2 e^{-|\alpha|^2} \cos \varphi + |\alpha|^2 + n \right), \\ E_2 &\equiv \langle a_1 a_2 \rangle = \frac{2}{(n-1)!} N_c^{-1} e^{-|\alpha|^2} \alpha^{n+1} \alpha^{*n-1} \cos \varphi, \\ E_3 &\equiv \langle a_1 \rangle = \langle a_2 \rangle \\ &= N_c^{-1} \left[\left(\frac{1}{(n-1)!} e^{-i\varphi} \alpha^{*n-1} + \frac{1}{n!} e^{i\varphi} \alpha \right) e^{-|\alpha|^2} |\alpha|^{2n} + \alpha \right]. \end{aligned} \tag{16}$$

Thus, we have

$$\begin{aligned} EPR &= 4E_1 - 8ReE_2 - 4Re(E_3^2 - 2E_2) \\ &\quad - 4Im(E_3^2 + 2E_2) + 1. \end{aligned} \tag{17}$$

It is shown that when $n = 0$, EPR is always less than 2. Using Eqs. (16) and (17), we plot the EPR as the function of φ with $n = 1, 2, 3$ in Fig. 2. It is obvious that when the relative phase φ is fixed, the value of EPR increases with the increase of photon number n , and finally exceeds $EPR > 2$.

Fig. 2 The EPR for the NAAN state as a function φ with $\alpha = 1$ and $n = 1, 2, 3$.



4 Quantum Statistical Distribution for the NAAN State

This section is subdivided into three subsections, i.e., Mandel Q-parameter, Wigner function and violation of the Clauser-Horne-Shimony-Holt (CHSH) inequality.

4.1 Mandel Q-Parameter

Mandel parameter ordinarily is defined as follows [47]

$$Q_M^k = \frac{\langle N_k^2 \rangle - \langle N_k \rangle^2}{\langle N_k \rangle} - 1, \tag{18}$$

where $N_k = a_k^\dagger a_k$ and $k = 1, 2$ indicates the 1 and 2 mode, respectively. Using $(a_k^\dagger a_k)^2 = a_k^{\dagger 2} a_k^2 + a_k^\dagger a_k$, we have

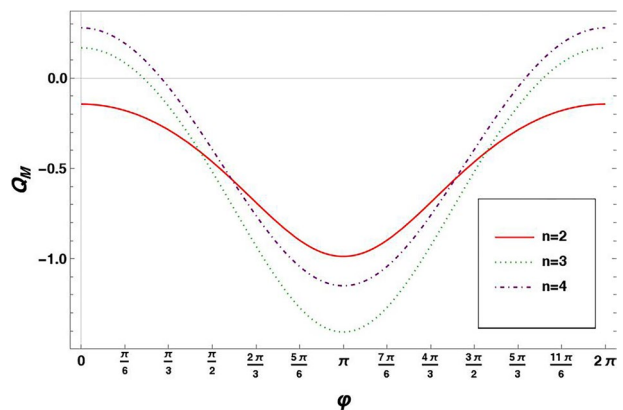
$$Q_M^k = \frac{\langle a_k^{\dagger 2} a_k^2 \rangle - \langle a_k^\dagger a_k \rangle^2}{\langle a_k^\dagger a_k \rangle}. \tag{19}$$

The average value of $a_k^{\dagger 2} a_k^2$ is

$$\begin{aligned} Q &\equiv \langle a_1^{\dagger 2} a_1^2 \rangle = \langle a_2^{\dagger 2} a_2^2 \rangle \\ &= N_c^{-1} \left[\frac{2}{(n-2)!} |\alpha|^{2n} e^{-|\alpha|^2} \cos \varphi + |\alpha|^4 + n(n-1) \right]. \end{aligned} \tag{20}$$

The negativity of Mandel parameter in Eq. (20) indicates that the quantum statistics is sub-Poissonian and shows the non-classicality of the state. Figure 3 shows that Q_M^k takes the minimum negative value at $\varphi = \pi$. Thus, the odd NAAN state has sub-Poissonian photon number distribution for $n = 2, 3, 4$. As α and n increase, we have $Q_M > 0$ which imply the non-classical quantum statistical effects of the NAAN state gradually disappear.

Fig. 3 The Q_M for the NAAN state as a function of φ with $\alpha = 1$ and $n = 2, 3, 4$.



4.2 Wigner Function

The negativity values in the Wigner function are major criteria on non-classicality of the quantum state [48, 49]. For analyzing the non-classicality of the NAAN state, one can use the definition of two-mode Wigner function as

$$W(\gamma_1, \gamma_2) = \frac{2}{\pi^2} e^{2(|\gamma_1|^2 + |\gamma_2|^2)} \int \frac{d^2z_1 d^2z_2}{\pi^2} \langle -z_1, -z_2 | \rho | z_1, z_2 \rangle e^{-2(z_1\gamma_1^* - z_1^*\gamma_1) - 2(z_2\gamma_2^* - z_2^*\gamma_2)}, \tag{21}$$

where in the phase space

$$\begin{aligned} \gamma_1 &= \frac{q_1 + ip_1}{\sqrt{2}}, & \gamma_2 &= \frac{q_2 + ip_2}{\sqrt{2}}, \\ q_{\pm} &= \frac{q_1 \pm q_2}{\sqrt{2}}, & p_{\pm} &= \frac{p_1 \pm p_2}{\sqrt{2}}. \end{aligned}$$

Substituting Eq. (1) into Eq. (21), one can finally obtain (see Appendix 2)

$$W(\gamma_1, \gamma_2) = \frac{2}{\pi^2} (-1)^n e^{-2(|\gamma_1|^2 + |\gamma_2|^2)} N_c^{-1} (F_1 + 2ReF_2 + F_3), \tag{22}$$

where

$$\begin{aligned} F_1 &= L_m(-4|\gamma_1|^2) \exp(2\alpha\gamma_2^* + 2\gamma_2\alpha^* - |\alpha|^2), \\ F_2 &= \frac{1}{n!} e^{i\varphi} (2\gamma_2 - \alpha)^n (\alpha^* - 2\gamma_1^*)^n \exp[2(\gamma_1\alpha + \alpha\gamma_2^*)], \\ F_3 &= L_n(-4|\gamma_2|^2) \exp(2\alpha\gamma_1^* + 2\gamma_1\alpha^* - |\alpha|^2). \end{aligned} \tag{23}$$

Comparing with Figs.4(a)-(c), it is not difficult to see that the negative values of Wigner function show that the NAAN states are the non-Gaussian quantum states. In addition, the maximum positive values of even NAAN states are greater than the absolute value of the maximum negative values, while the opposite is true of odd NAAN states. Therefore, from the perspective of quantum statistical distribution, the non-classical properties of odd NAAN states are more obvious than those of even NAAN states. Comparing Fig. 4. (b) and (d), the Wigner function does not change significantly. Thus, it can be seen that when the amplitude of coherent states α is fixed, the statistical distribution of quantum states mainly depends on the size of particle number n , and has little relationship with the relative phase φ .

4.3 Violation of the CHSH Inequality

In this subsection, we study the quantum nonlocality test for the NAAN state. Bell has proposed a remarkable inequality imposed by a local hidden variable theory, which enables a quantitative test on nonlocality of quantum states. For the two-mode case, the CHSH inequality based on the Wigner function is expressed as [50]

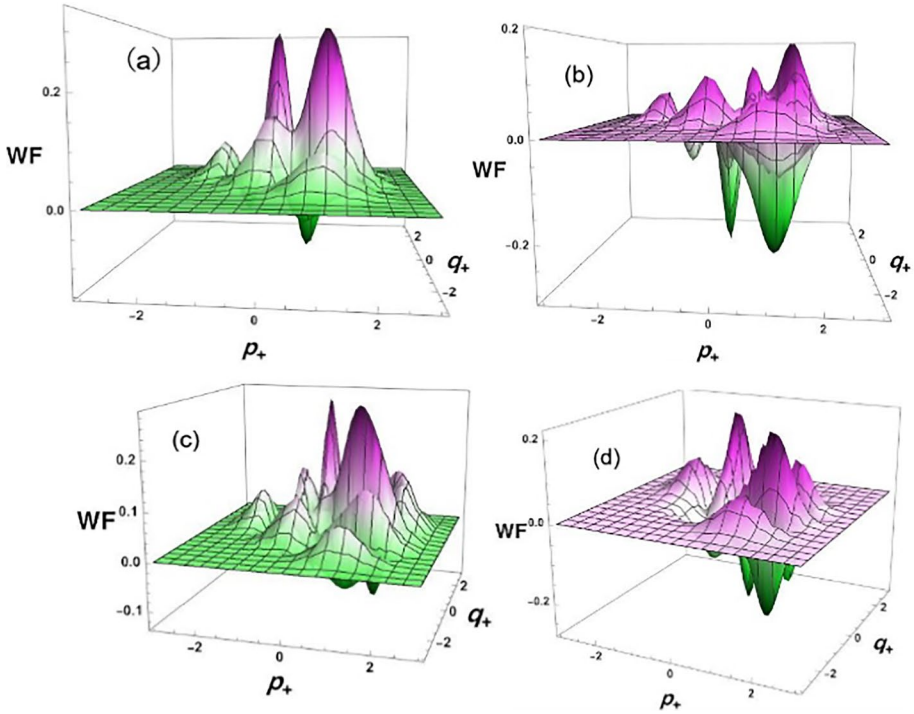


Fig. 4 The Wigner function in $q_+ - p_+$ phase space with $\alpha = 1$ where the values of (n, φ) are respectively (a) $(2, 0)$, (b) $(3, 0)$, (c) $(4, 0)$, (d) $(3, \pi)$

$$|B| = \frac{\pi^2}{4} \left| W(\gamma_1, \gamma_2) + W(\gamma_1, \gamma'_2) + W(\gamma'_1, \gamma_2) - W(\gamma'_1, \gamma'_2) \right| \leq 2. \tag{24}$$

Here by letting

$$\gamma_1 = 0, \gamma_2 = 0, \gamma'_1 = \sqrt{J}, \gamma'_2 = -\sqrt{J}, \tag{25}$$

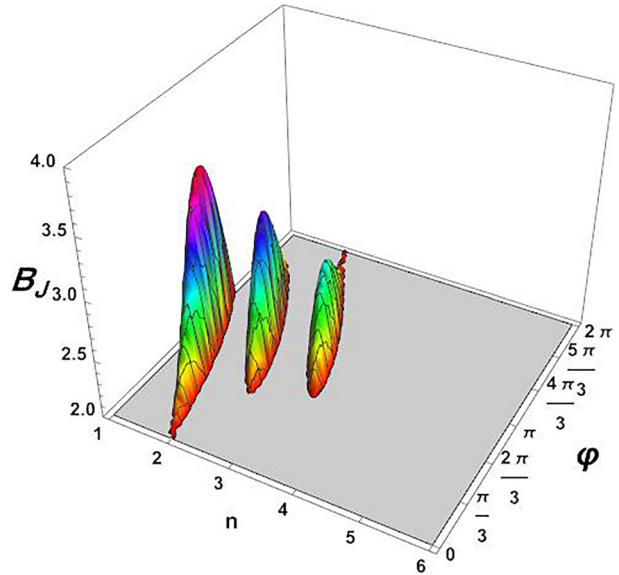
one has

$$|B_J| = \frac{\pi^2}{4} \left| W(0, 0) + W(\sqrt{J}, 0) + W(0, -\sqrt{J}) - W(\sqrt{J}, -\sqrt{J}) \right|, \tag{26}$$

where $J > 0$ is the magnitude of the displacement for the Bell test.

Using Eqs. (22) and (26), the numerical CHSH is obtained with the NAAN state, which are shown in Fig. 5. For $\varphi = \pi$, we find much stronger violations of the CHSH in the regime $1 \leq n \leq 3$. For $\varphi = 0, 2\pi$, we find violations of the inequality only at $n = 2$. In other cases $0 < \varphi < \pi$ and $\pi < \varphi < 2\pi$, the violations of the inequality obtained with the NAAN state occur over a range of photon numbers $1 \leq n \leq 3$. In addition, the violation of the CHSH inequality diminishes for increasing n . The most interesting result is with respect to the CHSH inequality which for the NOON states is violated only for case $n = 1$, whereas for the NAAN state increasing violations at a wider range of photon numbers $n > 1$.

Fig. 5 The CHSH quantity $|B_J|$ as a function of n and φ with $J = 0.1$ and $\alpha = 1.5$.



5 Phase Measurement via Parity Detection

Quantum phase measurement plays a very important role in quantum metrology, because it can help us determine how small the accuracy of the phase we can detect. It has been reported that quantum vacuum state can be estimated with an error $\Delta\varphi \sim 1/\sqrt{N}$, which is just the so-called standard quantum limit. Some nonclassical states and the entangled states, such as NOON states and two-mode squeezed vacuum state, can reach the Heisenberg limit $\Delta\varphi \sim 1/N$ in a photon lossless environmental measurement. There are three types of detection schemes to measure the phase information of the quantum state, i.e., homodyne detection, intensity detection and parity detection. In section, we focus on the parity detection and the classical Fisher information.

5.1 Parity Detection with the NAAN State

The purpose of parity detection is to obtain the average value of parity operators in the quantum state, which has many applications in Wigner function and phase measurement [51–53]. Here, we take the parity operator of mode 1 as

$$\Pi_1 = (-1)^{a_1^\dagger a_1} = \int \frac{d^2\gamma_1}{\pi} |\gamma_1\rangle\langle -\gamma_1|, \tag{27}$$

where $|\gamma_1\rangle$ is the normal coherent state.

Using the eigen-equation of parity operator $\Pi_1|N_1\rangle = (-1)^n|N_1\rangle$ and $\Pi_1|\alpha_1\rangle = |-\alpha_1\rangle$, the expectation value of the parity operator for the NAAN state is

$$\langle \Pi_1 \rangle = N_c^{-1} \left[\frac{2}{n!} (-1)^n |\alpha|^{2n} e^{-|\alpha|^2} \cos \varphi + e^{-2|\alpha|^2} + (-1)^n \right]. \tag{28}$$

It can be seen from the Fig. 6(a) that the average value of parity operator decreases continuously with the increase of α . The average values parity operator is $\langle \Pi_1 \rangle \leq 0$ when n is odd, but greater than zero when n is even in the case $\varphi = 0$. Comparing Figs.6(b)-(c), it is clear to see that the trough or peak of the curve occurs in $\varphi = \pi$. In addition, the central trough of $n = 0$ is narrower than that of $n = 1, 2$ under the same parameters. In the case of $n = 0, 1$, the phase sensitivity of parity measurement increases with the increase of α , but in the case of $n = 2$, it is opposite. Therefore, to obtain the best phase measurement sensitivity for the NAAN state, the measurement objects are the quantum states with the relative phase $\varphi = \pi$ and small n and α values, especially $n = 0, \alpha \rightarrow 0$.

5.2 Classical Fisher Information

After investigating the expectation values of the parity operator, in this subsection, we further consider the classical Fisher information (CFI) based on parity detection in Eq. (28). In general, the CFI can be estimated as [54, 55]

$$F_c = \frac{\left| \frac{\partial}{\partial \varphi} \langle \Pi_1 \rangle \right|^2}{\Delta^2 \Pi_1} = \frac{\left| \frac{\partial}{\partial \varphi} \langle \Pi_1 \rangle \right|^2}{1 - \langle \Pi_1 \rangle^2}, \tag{29}$$

where we have used

$$\Delta^2 \Pi_1 \equiv \langle \Pi_1^2 \rangle - \langle \Pi_1 \rangle^2 = 1 - \langle \Pi_1 \rangle^2. \tag{30}$$

Using Eq. (28), one obtain

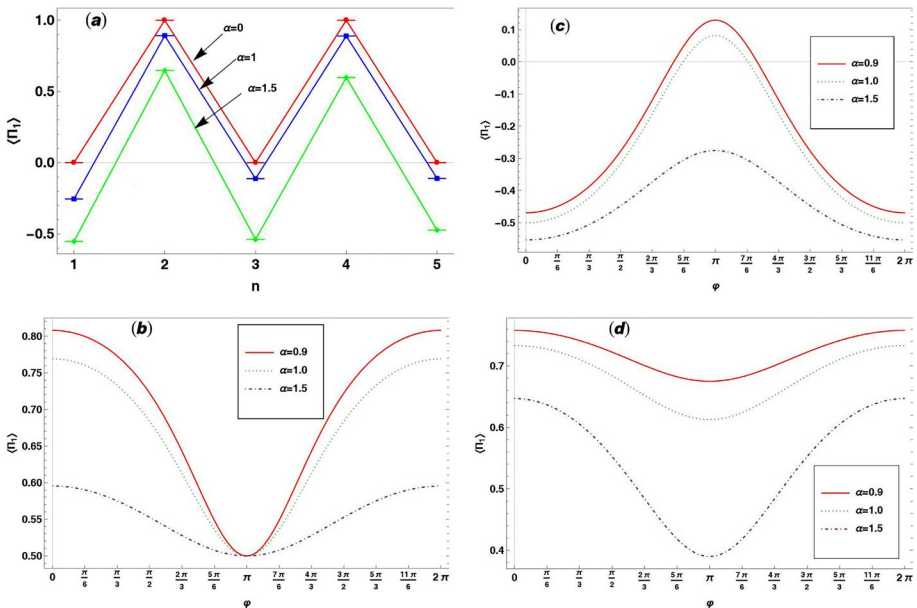


Fig. 6 a The average value of parity operator as a function of n with $\alpha = 0, 1, 1.5$ and $\varphi = 0$. $\langle \Pi_1 \rangle$ as function of φ with $\alpha = 0.9, 1.0, 1.5$ and **b** $n = 0$, **c** $n = 1$, **d** $n = 2$.

$$\frac{\partial}{\partial \varphi} \langle \Pi_1 \rangle = - \frac{(e^{|\alpha|^2} - 1) |\alpha|^4 \sin \varphi}{(2e^{|\alpha|^2} + |\alpha|^4 \cos \varphi)^2}. \tag{31}$$

Substituting Eqs. (28) and (31) into (29), the CFI for the NAAN states is obtained

$$F_c = \frac{\left| K \left[(-1)^n e^{|\alpha|^2} - 1 \right] |\alpha|^{2n} n! \sin \varphi \right|^2}{\left| K \left(2(-1)^n |\alpha|^{2n} \cos \varphi + n! + n! (-1)^n e^{|\alpha|^2} \right)^2 \right| - 4} \tag{32}$$

where

$$K = \frac{1}{(|\alpha|^{2n} \cos \varphi + e^{|\alpha|^2} n!)^2}. \tag{33}$$

The phase sensitivity of the NAAN state can be estimated by the error propagation formula as

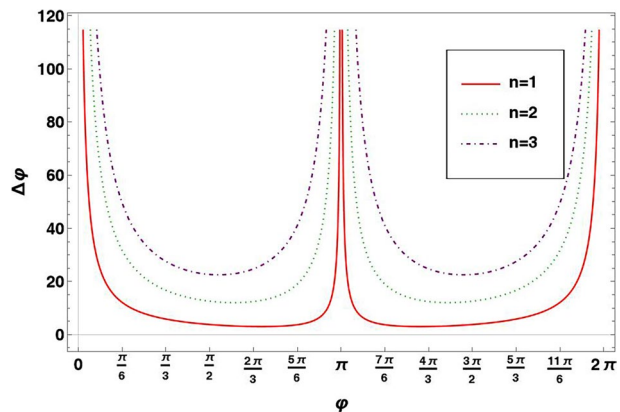
$$\Delta \varphi = \frac{1}{\sqrt{F_c}}. \tag{34}$$

From Fig. 7, it is easy to see that the phase fluctuation $\Delta \varphi$ is the largest at $\varphi = 0, \pi, 2\pi$. The minimum phase fluctuation is in the range of $5\pi/6 < \varphi < \pi$ or $\pi < \varphi < 7\pi/6$. In addition, at the same phase φ , the phase uncertainty $\Delta \varphi$ increases with the increase of photon number n . Furthermore, when the amplitude of the coherent state α tends to zero, the quantum phase fluctuation also tends to zero, even reaching the Heisenberg limit $\Delta \varphi = 1/N$.

6 Squeezing Properties

The investigation of the squeezing effects of the quantum states is of considerable interest since it plays an important role in the quantum theory [56, 57]. There are several different methods used to analyze the squeezing properties of two-mode quantum states, such as sum

Fig. 7 The phase uncertainty $\Delta \varphi$ as a function of φ with $\alpha = 1$ and $n = 1, 2, 3$.



squeezing, difference squeezing, quadrature squeezing, amplitude-squared squeezing. In principle, it has been studied that sum squeezing can be converted into normal single-mode squeezing using the sum-frequency generation. Therefore, in this section we focus on the sum squeezing and different squeezing properties of the NAAN states.

6.1 Sum Squeezing

For two-mode quantum state, the sum squeezing is associated with a more general operator [58]

$$V_\theta = \frac{1}{2} \left(e^{i\theta} a_1^\dagger a_2^\dagger + e^{-i\theta} a_1 a_2 \right). \quad (35)$$

A state is said to be sum squeezed if

$$S_\theta \equiv \left\langle (\Delta V_\theta)^2 \right\rangle - \frac{1}{4} \langle N_1 + N_2 + 1 \rangle < 0, \quad (36)$$

where $\left\langle (\Delta V_\theta)^2 \right\rangle = \langle V_\theta^2 \rangle - \langle V_\theta \rangle^2$, $N_1 = a_1^\dagger a_1$ and $N_2 = a_2^\dagger a_2$

We define the squeezing factor to quantify the squeezing degree of sum squeezing as

$$S = \frac{4S_\theta}{\langle N_1 + N_2 + 1 \rangle}, \quad (37)$$

which is bounded by $-1 \leq S < 0$ for the case of sum squeezing occurs. It is clear to see that the closer S trends to -1 , the higher the degree of sum squeezing.

Substituting Eq. (35) into Eq. (37), we can rewrite Eq. (37) as

$$S = \frac{2 \left[\operatorname{Re} \left(e^{-2i\theta} \langle a_1^2 a_2^2 \rangle \right) - 2 \operatorname{Re}^2 \left(e^{-i\theta} \langle a_1 a_2 \rangle \right) + \left\langle a_1^\dagger a_1 a_2^\dagger a_2 \right\rangle \right]}{\left\langle a_1^\dagger a_1 \right\rangle + \left\langle a_2^\dagger a_2 \right\rangle + 1}, \quad (38)$$

where $\operatorname{Re}(z)$ is the real part of a complex number z .

Expectation values of $\langle a_1^2 a_2^2 \rangle$ and $\langle a_1^\dagger a_1 a_2^\dagger a_2 \rangle$ are

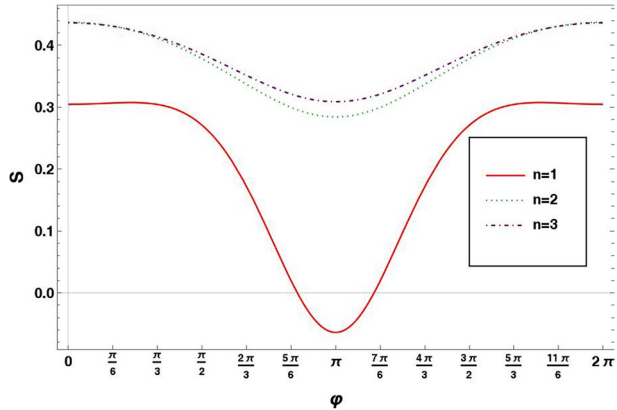
$$\langle a_1^2 a_2^2 \rangle = N_c^{-1} \frac{1}{(n-2)!} 2\alpha^{n+2} \alpha^{*n-2} e^{-|\alpha|^2} \cos \varphi, \quad (39)$$

and

$$\langle a_1^\dagger a_1 a_2^\dagger a_2 \rangle = 2N_c^{-1} \left(\frac{|\alpha|^{2n}}{n!} n^2 e^{-|\alpha|^2} \cos \varphi + n|\alpha|^2 \right) \quad (40)$$

Substituting Eqs. (16), (39) and (40) into (38), We plot in Fig. 8 the sum squeezing degree S as a function of the relative phase φ with $n = 1, 2, 3$ and $\theta = 0, \alpha = 1.5$. What stands out in Fig. 8 is that the NAAN state exhibits a maximum degree of sum squeezing under $n = 1$ and $\varphi = \pi$ conditions. Visually, S becomes positive when $n > 2$ for any φ , which means no sum squeezing arises at all. For $n = 1$, when S is negative, φ is in the range $5\pi/6 < \varphi < 7\pi/6$.

Fig. 8 The sum squeezing degree S as a function of φ with $n = 1, 2, 3$ and $\theta = 0, \alpha = 1.5$.



6.2 Difference Squeezing

For the two-mode state, difference squeezing is associated with the operator W_θ [58]

$$W_\theta = \frac{1}{2} \left(e^{i\theta} a_1 a_2^\dagger + e^{-i\theta} a_1^\dagger a_2 \right). \tag{41}$$

A state is said to be difference squeezed along a direction θ if

$$\langle (\Delta W_\theta)^2 \rangle < \frac{1}{4} |\langle N_1 - N_2 \rangle|. \tag{42}$$

Noting $\langle (\Delta W_\theta)^2 \rangle = \langle W_\theta^2 \rangle - \langle W_\theta \rangle^2$ and $\langle N_1 \rangle = \langle N_2 \rangle$ for the NAAN state??we can rewrite Eq. (42) as

$$\begin{aligned} \langle (\Delta W_\theta)^2 \rangle &= 2Re \left(e^{2i\theta} \langle a_1^2 a_2^{\dagger 2} \rangle \right) - 4 \left[Re \left(e^{i\theta} \langle a_1 a_2^\dagger \rangle \right) \right]^2 \\ &+ 2 \langle a_1^\dagger a_1 a_2^\dagger a_2 \rangle + \langle a_1 a_1^\dagger \rangle + \langle a_2 a_2^\dagger \rangle < 0. \end{aligned} \tag{43}$$

The expected values of operators $a_1 a_2^\dagger$ and $a_1^2 a_2^{\dagger 2}$ are

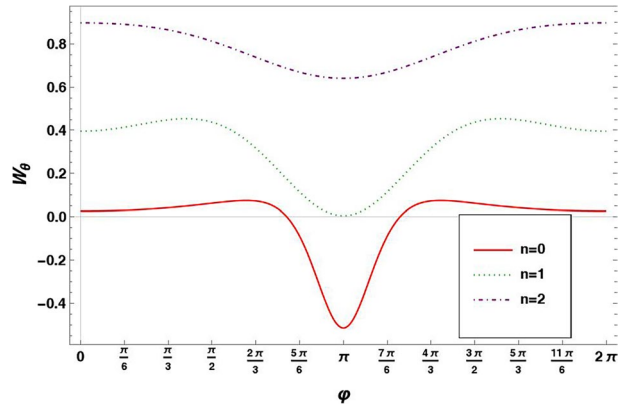
$$\langle a_1 a_2^\dagger \rangle = N_c^{-1} \frac{1}{n!} |\alpha|^{2n} e^{-|\alpha|^2} (n^2 |\alpha|^{-2} e^{-i\varphi} + \alpha^* e^{i\varphi}), \tag{44}$$

and

$$\begin{aligned} \langle a_1^2 a_2^{\dagger 2} \rangle &= N_c^{-1} |\alpha|^{2n} e^{-|\alpha|^2} \\ &\left(e^{-i\varphi} |\alpha|^{-4} \frac{n}{(n-3)!} + e^{i\varphi} |\alpha|^4 \sqrt{\frac{(n+1)}{n!(n+3)!}} \right). \end{aligned} \tag{45}$$

We can see from Fig. 9 that $\langle (\Delta W_\theta)^2 \rangle$ have the smallest value at $\varphi = \pi$. In addition, $\langle (\Delta W_\theta)^2 \rangle$ as a function of φ kept positive when $n = 1, 2$. Thus, we find that the difference squeezing exists only with $n = 0$.

Fig. 9 The $\langle (\Delta W_\theta)^2 \rangle$ as a function of φ with $n = 0, 1, 2$ and $\theta = \pi, \alpha = 0.5$.



7 Conclusion

We have proposed a new symmetric hybrid state which is composed by two discrete Fock number states $|N\rangle$ and two continuous coherent states $|\alpha\rangle$ in two-mode state with an arbitrary phase angle φ . We found that this state can be considered as the superpositions of NOON states. Therefore, in the case of $\varphi = 0, \pi$ and $\alpha = 1$, it is different from the normal Bell state.

Evaluating the degree of entanglement of the NAAN states, our results suggest that the even NAAN state ($\varphi = 0, 2\pi$) has a high degree of entanglement. To rigorously discuss entanglement, EPR criterion was used to analyze entanglement of the NAAN states. It is shown that when $n = 0$, the NAAN states are always entangled which no dependence on the parameters φ and α . Specifically, when $n > 3$, the NAAN states no longer exhibit entangled properties.

Entanglement, non-Gaussian distribution and non-locality are typical properties of non-classical quantum states. Interestingly, through the analysis of Mandel parameter, we find that the odd NAAN states have sub-Poissonian photon number distribution for $n = 2, 3, 4$. Further, the conclusion is confirmed by the analysis of Wigner function. Some strong violations of the CHSH inequality at a wider range of photon numbers $n = 1, 2, 3$ were also found.

The relative phase φ of the NAAN states can be considered as a phase-shift parameter between two-arm in a linear Mach–Zehnder interferometer. Thus, through the numerical analysis of parity detection, we find that the best phase measurement sensitivity is obtained when $\varphi = \pi$ and small values of n and α , especially $n = 0, \alpha \rightarrow 0$. Furthermore, when the amplitude of the coherent state α tends to zero, the quantum phase fluctuation also tends to zero, even reaching the Heisenberg limit $\Delta\varphi = 1/N$.

The theoretical discussions on sum squeezing show that only when $n = 1$ and $\alpha = 0.56$, sum squeezing of the NAAN state arise in the range $5\pi/6 < \varphi < 7\pi/6$. However, the difference squeezing exists only with $n = 0$ and $\alpha = 0.5$ in the range $5\pi/6 < \varphi < 7\pi/6$. In summary, the NAAN do not have the properties of sum squeezing and difference squeezing, when $n > 1$.

Hofmann and Ono have used the quantum interference between down-converted photon pairs and photons from coherent laser light to produce a path entangled multiphoton output state NOON [59]. Thus, the NAAN states may be realized in the same experimental settings. This is an important issue for future work.

Appendix 1. Derivation of expectation values in Eq. (16)

Using Eq. (1), the average value of the $a_1^\dagger a_1$ is

$$\begin{aligned} \langle a_1^\dagger a_1 \rangle &= N_c^{-1} (\langle N_2 | \langle \alpha_1 | e^{-i\varphi} + \langle \alpha_2 | \langle N_1 | \rangle a_1^\dagger a_1 (|N_1\rangle | \alpha_2 \rangle + e^{i\varphi} | \alpha_1 \rangle | N_2 \rangle)) \\ &= N_c^{-1} (\langle \alpha_2 | \alpha_2 \rangle \langle N_1 | a_1^\dagger a_1 | N_1 \rangle + \langle N_2 | N_2 \rangle \langle \alpha_1 | a_1^\dagger a_1 | \alpha_1 \rangle \\ &+ e^{i\varphi} \langle \alpha_2 | N_2 \rangle \langle N_1 | a_1^\dagger a_1 | \alpha_1 \rangle + e^{-i\varphi} \langle N_2 | \alpha_2 \rangle \langle \alpha_1 | a_1^\dagger a_1 | N_1 \rangle). \end{aligned} \tag{A1}$$

According $a|\alpha\rangle = \alpha|\alpha\rangle, a^\dagger a|n\rangle = n|n\rangle$ and $\langle \alpha | n \rangle = \frac{\alpha^n}{\sqrt{n!}} e^{-\frac{1}{2}|\alpha|^2}$, we have

$$\langle a_1^\dagger a_1 \rangle = N_c^{-1} \left(\frac{2}{(n-1)!} |\alpha|^2 e^{-|\alpha|^2} \cos \varphi + |\alpha|^2 + n \right). \tag{A2}$$

In a similar way, one readily obtain the average values of $a_2^\dagger a_2, a_1 a_2, a_1$ and a_2 as shown in Eq. (16).

Appendix 2. Derivation of Wigner function in Eq. (22)

We first calculate the inner product part of the Wigner function as

$$\begin{aligned} &\langle -z_1, -z_2 | \rho | z_1, z_2 \rangle \\ &= N_c^{-1} \langle -z_1, -z_2 | (|N_1\rangle | \alpha_2 \rangle + e^{i\varphi} | \alpha_1 \rangle | N_2 \rangle) \\ &(\langle N_2 | \langle \alpha_1 | e^{-i\varphi} + \langle \alpha_2 | \langle N_1 | \rangle | z_1, z_2 \rangle) \\ &= N_c^{-1} \frac{1}{n!} (-1)^n \left[z_1^{*n} z_1^n e^{-|z_1|^2 - |z_2|^2 - \alpha z_2^* + \alpha^* z_2} + z_2^{*n} z_2^n e^{-|z_1|^2 - |z_2|^2 - z_1^* \alpha + \alpha^* z_1} \right. \\ &\left. + e^{i\varphi} z_1^n z_2^{*n} e^{-|z_1|^2 - |z_2|^2 - \alpha z_1^* + \alpha z_2^*} + e^{-i\varphi} (z_1^*)^n z_2^n e^{-|z_1|^2 - |z_2|^2 + \alpha^* z_1 - \alpha z_2^*} \right], \end{aligned} \tag{B1}$$

where the overlap between two coherent states $\langle \alpha | \beta \rangle = \exp \left[-\frac{1}{2} (|\alpha|^2 + |\beta|^2) + \alpha^* \beta \right]$ has been used.

Using the definition of the Wigner function in Eq. (20), the first integral term is obtained as

$$\begin{aligned} F'_1 &= \frac{(-1)^n}{n!} \frac{2e^2 (|\gamma_1|^2 + |\gamma_2|^2)}{\pi^2} N_c^{-1} \int \frac{d^2 z_1 d^2 z_2}{\pi^2} z_1^{*n} z_1^n e^{-\alpha z_2^* + \alpha^* z_2} e^{-|z_1|^2 - |z_2|^2} \\ &\cdot \exp \left[2(z_1^* \gamma_1 - z_1 \gamma_1^*) + 2(z_2^* \gamma_2 - z_2 \gamma_2^*) \right] \\ &= \frac{(-1)^n}{n!} \frac{2e^2 (|\gamma_1|^2 + |\gamma_2|^2)}{\pi^2} N_c^{-1} \int \frac{d^2 z_1}{\pi} z_1^{*n} z_1^n \exp \left(-|z_1|^2 + 2z_1^* \gamma_1 - 2z_1 \gamma_1^* \right) \\ &\cdot \int \frac{d^2 z_2}{\pi} \exp \left[-|z_2|^2 + (2\gamma_2 - \alpha) z_2^* + (\alpha^* - 2\gamma_2^*) z_2 \right] \\ &= \frac{2}{\pi^2} e^{-2(|\gamma_1|^2 + |\gamma_2|^2)} (-1)^n N_c^{-1} L_m \left(-4|\gamma_1|^2 \right) \exp \left(2\alpha \gamma_2^* + 2\gamma_2 \alpha^* - |\alpha|^2 \right), \end{aligned} \tag{B2}$$

where we have used the integral formula of complex function

$$\int \frac{d^2z}{\pi} z^m z^{*m} \exp(-|z|^2 + \xi z + \eta z^*) = m! e^{\xi\eta} L_m(\xi\eta), \quad (\text{B3})$$

and

$$\int \frac{d^2z}{\pi} \exp(\zeta|z|^2 + \xi z + \eta z^*) = -\frac{1}{\zeta} \exp\left(-\frac{\xi\eta}{\zeta}\right), \quad \text{Re}(\xi) < 0. \quad (\text{B4})$$

Similarly, using Eqs. (22) and (B1) and the integral formula

$$\begin{aligned} \int \frac{d^2z}{\pi} z^n \exp(-|z|^2 + \xi z + \eta z^*) &= \eta^n e^{\xi\eta}, \\ \int \frac{d^2z}{\pi} z^{*n} \exp(-|z|^2 + \xi z + \eta z^*) &= \xi^n e^{\xi\eta}, \end{aligned} \quad (\text{B5})$$

we have

$$\begin{aligned} F'_2 &= e^{-i\varphi} \frac{(-1)^n}{n!} \frac{2e^{2(|\gamma_1|^2 + |\gamma_2|^2)}}{\pi^2} N_c^{-1} \\ &\int \frac{d^2z_1 d^2z_2}{\pi^2} z_1^{*n} z_2^n e^{-|z_1|^2 - |z_2|^2 - \alpha z_1^* + \alpha^* z_1} \\ &\exp\left[2(z_1^* \gamma_1 - z_1 \gamma_1^*) + 2(z_2^* \gamma_2 - z_2 \gamma_2^*)\right] \\ &= e^{-i\varphi} \frac{(-1)^n}{n!} \frac{2e^{-2(|\gamma_1|^2 + |\gamma_2|^2)}}{\pi^2} N_c^{-1} \\ &(2\gamma_2 - \alpha)^n (\alpha^* - 2\gamma_1^*)^n \exp(2\gamma_1 \alpha + 2\alpha \gamma_2^*) \end{aligned} \quad (\text{B6})$$

and

$$\begin{aligned} F'_3 &= \frac{(-1)^n}{n!} \frac{2e^{2(|\gamma_1|^2 + |\gamma_2|^2)}}{\pi^2} N_c^{-1} \int \frac{d^2z_1 d^2z_2}{\pi^2} z_2^n z_2^{*n} e^{-\alpha z_1^*} e^{\alpha^* z_1} \\ &\exp\left[2(z_1^* \gamma_1 - z_1 \gamma_1^*) + 2(z_2^* \gamma_2 - z_2 \gamma_2^*)\right] \\ &= \frac{(-1)^n}{n!} \frac{2}{\pi^2} e^{-2(|\gamma_1|^2 + |\gamma_2|^2)} N_c^{-1} \\ &n! L_n(4|\gamma_2|^2) \exp(2\alpha \gamma_1^* + 2\gamma_1 \alpha^* - |\alpha|^2) \end{aligned} \quad (\text{B7})$$

Substituting Eqs.(B2),(B6) and (B7) into (20) and after some simplifications, Eq. (22) is obtained.

Author contributions Gang Ren and Haijun Yu wrote the main manuscript text and Chun-zao Zhang and Feng Chen prepared figures 1-9. All authors reviewed the manuscript.

Funding This work is supported by the Natural Science Foundation of the Anhui Higher Education Institutions of China (Grant No. 2022AH051580) and the University Synergy Innovation Program of Anhui Province (Grant No. GXXT-2022-050).

Declarations

Competing interests The authors declare no competing interests.

References

- van Enk, S.J., Hirota, O.: Entangled coherent states: Teleportation and decoherence. *Phys Rev A* **64**(2), 022313–1–6 (2001)
- Dodonov, V.V.: “Nonclassical” states in quantum optics: a “squeezed” review of the first 75 years. *J Opt B-Quantum S O* **4**(1), R1–R33 (2002)
- Mojaveri, B., Dehghani, A., JafarzadehBahrbeig, R.: Enhancing entanglement of entangled coherent states via a f-deformed photon-addition operation. *Eur Phys J Plus* **134**(9), 456–1–8 (2019)
- Liu, C., Yu, M., Ye, W., Zhang, H., Hu, L.: Preparation of nonclassical states by displacement-based quantum scissors. *Results Phys* **19**, 103616–1–6 (2020)
- Matia-Hernando, P., Luis, A.: Nonclassicality in phase-number uncertainty relations. *Phys Rev A* **84**(6), 063829–1–7 (2011)
- Dehghani, A., Mojaveri, B., Alenabi, A.A.: Entangled nonlinear coherent-squeezed states: inhibition of depolarization and disentanglement. *Appl Phys B* **128**(2), 23–1–10 (2022)
- Anbaraki, A., Afshar, D., Jafarpour, M.: Non-classical properties and polarization degree of photon-added entangled nonlinear coherent states. *Eur Phys J Plus* **133**(1), 2–1–11 (2018)
- Dehghani, A., Mojaveri, B., Aryaie, M.: Nonclassical properties and polarization degree of photon-subtracted entangled nonlinear coherent states. *Int J Mod Phys B* **33**(21), 1950230 (2019)
- Bose, S., Kumar, M.S.: Analysis of necessary and sufficient conditions for quantum teleportation with non-Gaussian resources. *Phys Rev A* **103**(3), 032432–1–5 (2021)
- Mojaveri, B., Dehghani, A., JafarzadehBahrbeig, R.: Nonlinear coherent states of the para-Bose oscillator and their non-classical features. *Eur Phys J Plus* **133**(12), 529–1–16 (2018)
- Mojaveri, B., Dehghani, A., Faseghandis, S.A.: Even and odd λ -deformed binomial states: minimum uncertainty states. *Eur Phys J Plus* **132**(3), 128–1–9 (2017)
- Dai, Q., Jing, H.: Photon-Added Entangled Coherent State. *Int J Theor Phys* **47**(10), 2716–2721 (2008)
- Lee, S.Y., Park, J., Lee, H.W., Nha, H.: Generating arbitrary photon-number entangled states for continuous-variable quantum informatics. *Opt Express* **20**(13), 14221–14233 (2012)
- Gomez, E.S., Nogueira, W.A.T., Monken, C.H., Lima, G.: Quantifying the non-Gaussianity of the state of spatially correlated down-converted photons. *Opt Express* **20**(4), 3753–3772 (2012)
- Lee, J., Kim, J., Nha, H.: Demonstrating higher-order nonclassical effects by photon-added classical states: realistic schemes. *J Opt Soc Am B* **26**(7), 1363–1369 (2009)
- Ben-Aryeh, Y.: Phase estimation by photon counting measurements in the output of a linear Mach-Zehnder interferometer. *J Opt Soc Am B* **29**(10), 2754–2764 (2012)
- Sivakumar, S.: Photon-added coherent states in parametric down-conversion. *Phys Rev A* **83**(3), 035802–1–4 (2011)
- Takeda, S., Benichi, H., Mizuta, T., Lee, N., Yoshikawa, J., Furusawa, A.: Quantum mode filtering of non-Gaussian states for teleportation-based quantum information processing. *Phys Rev A* **85**(5), 053824–1–7 (2012)
- Solano, E., Agarwal, G.S., Walther, H.: Generalized Schrodinger cat states in cavity QED. *Opt. Spectrosc.* **94**(5), 805–807 (2003)
- Xiang, S.-H., Song, K.-H.: Quantum non-Gaussianity of single-mode Schrödinger cat states based on Kurtosis. *Eur Phys J D* **69**(11), 260–1–9 (2015)
- Filip, R.: Gaussian quantum adaptation of non-Gaussian states for a lossy channel. *Phys Rev A* **87**(4), 042308–1–6 (2013)
- Joo, J., Elliott, M., Oi, D.K.L., Ginossar, E., Spiller, T.P.: Deterministic amplification of Schrödinger cat states in circuit quantum electrodynamics. *New J Phys* **18**(2), 023028–1–10 (2016)
- Dehghani, A., Mojaveri, B., Aryaie, M., Alenabi, A.A.: Superposition of two-mode “Near” coherent states: non-classicality and entanglement. *Quantum Inf Process* **18**(5), 148–1–6 (2019)
- Karimi, A., Tavassoly, M.K.: Single-mode nonlinear excited entangled coherent states and their nonclassical properties. *Phys Scripta* **90**(1), 015101–1–14 (2015)
- Lee, C.W., Ji, S.W., Nha, H.: Quantum steering for continuous-variable states. *J Opt Soc Am B* **30**(9), 2483–2490 (2013)
- Dowling, P.: Quantum optical metrology - the lowdown on high-NOON states. *Contemp. Phys.* **49**(2), 125–143 (2008)
- Giovannetti, V., Lloyd, S., Maccone, L.: Quantum-Enhanced Measurements: Beating the Standard Quantum Limit. *Science* **306**(5700), 1330–1336 (2004)
- Xu, X.X., Yuan, H.C.: Quantum phase estimation with local amplified 1001 state based on Wigner-function method. *Quantum Inf Process* **14**(1), 411–424 (2015)
- Kim, H., Park, H.S., Choi, S.K.: Three-photon NOON states generated by photon subtraction from double photon pairs. *Opt Express* **17**(22), 19720–19726 (2009)

30. Boto, A.N., Kok, P., Abrams, D.S., Braunstein, S.L., Williams, C.P., Dowling, J.P.: Quantum interferometric optical lithography: Exploiting entanglement to beat the diffraction limit. *Phys Rev Lett* **85**(13), 2733–2736 (2000)
31. Gilbert, G., Hamrick, M., Weinstein, Y.S.: Use of maximally entangled N-photon states for practical quantum interferometry. *J Opt Soc Am B* **25**(8), 1336–1340 (2008)
32. Mirza, I.M., Cruz, A.S.: On the dissipative dynamics of entangled states in coupled-cavity quantum electrodynamics arrays. *J Opt Soc Am B* **39**(1), 177–187 (2022)
33. Afek, I., Ambar, O., Silberberg, Y.: High-NOON States by Mixing Quantum and Classical Light. *Science* **328**(5980), 879–881 (2010)
34. Li, Y., Jing, H., Zhan, M.S.: Optical generation of a hybrid entangled state via an entangling single-photon-added coherent state. *J Phys B-at Mol Opt* **39**(9), 2107–2113 (2006)
35. Nagali, E., Sciarrino, F.: Generation of hybrid polarization-orbital angular momentum entangled states. *Opt Express* **18**(17), 18243–18248 (2010)
36. Shukla, C., Malpani, P., Thapliyal, K.: Hierarchical Quantum Network using Hybrid Entanglement. *Quantum Inf Process* **20**(3), 121–1–19 (2021)
37. Kreis, K., van Loock, P.: Classifying, quantifying, and witnessing qudit-qumode hybrid entanglement. *Phys Rev A* **85**(3), 032307-1–14 (2012)
38. dSouza, A.D., Cardoso, W.B., Avelar, A.T., Baseia, B.: Teleportation of entangled states without Bell-state measurement via a two-photon process. *Opt Commun* **284**(4), 1086–1089 (2011)
39. Jennewein, T., Weihs, G., Zeilinger, A.: Photon Statistics and Quantum Teleportation Experiments. *J Phys Soc Jpn* **72**, 168–173 (2003)
40. Gaspard, P.: Entropy production in the quantum measurement of continuous observables. *Phys Lett A* **377**(3–4), 181–184 (2013)
41. Cardy, J.L.: Entanglement entropy in extended quantum systems. *Eur Phys J B* **64**(3–4), 321–326 (2008)
42. Gillet, J., Bastin, T., Agarwal, G.S.: Multipartite entanglement criterion from uncertainty relations. *Phys Rev A* **78**(5), 052317-1–5 (2008)
43. McKinstrie, C.J., Karlsson, M.: Schmidt decompositions of parametric processes I: Basic theory and simple examples. *Opt Express* **21**(2), 1374–1394 (2013)
44. Gerry, C.C., Mimih, J., Benmoussa, A.: Maximally entangled coherent states and strong violations of Bell-type inequalities. *Phys Rev A* **80**(2), 022111-1–11 (2009)
45. Eberhard, P.H., Rosselet, P.: Bells theorem based on a generalized EPR criterion of reality. *Found. Phys.* **25**(1), 91–111 (1995)
46. Cavalcanti, E.G., Jones, S.J., Wiseman, H.M., Reid, M.D.: Experimental criteria for steering and the Einstein-Podolsky-Rosen paradox. *Phys Rev A* **80**(3), 032112-1–16 (2009)
47. Mandel, L.: Squeezed States and Sub-Poissonian Photon Statistics. *Phys Rev Lett* **49**(2), 136–138 (1982)
48. Ferrie, C.: Quasi-probability representations of quantum theory with applications to quantum information science. *Rep Prog Phys* **74**(11), 116001-1–24 (2011)
49. Veitch, V., Ferrie, C., Gross, D., Emerson, J.: Negative quasi-probability as a resource for quantum computation. *New J Phys* **14**, 113011-1–21 (2012)
50. Sponar, S., Klepp, J., Zeiner, C., Badurek, G., Hasegawa, Y.: Violation of a Bell-like inequality for spin-energy entanglement in neutron polarimetry. *Phys Lett A* **374**(3), 431–434 (2010)
51. Chiruvelli, A., Lee, H.: Parity measurements in quantum optical metrology. *J Mod Optic* **58**(11), 945–953 (2011)
52. Seshadreesan, K.P., Kim, S., Dowling, J.P., Lee, H.: Phase estimation at the quantum Cramér-Rao bound via parity detection. *Phys Rev A* **87**(4), 043833-1–6 (2013)
53. Hu, L.Y., Wei, C.P., Huang, J.H., Liu, C.J.: Quantum metrology with Fock and even coherent states: Parity detection approaches to the Heisenberg limit. *Opt Commun* **323**, 68–76 (2014)
54. Liu, C.-C., Wang, D., Sun, W.-Y., Ye, L.: Quantum Fisher information, quantum entanglement and correlation close to quantum critical phenomena. *Quantum Inf Process* **16**(9), 219–1–15 (2017)
55. Ren, Z.H., Li, Y., Li, Y.N., Li, W.D.: Development on quantum metrology with quantum Fisher information. *Acta Phys Sin-Ch Ed* **68**(4), 040601-1–30 (2019)
56. Missori, R.J., de Oliveira, M.C., Furuya, K.: Non-Gaussian two-mode squeezing and continuous-variable entanglement of linearly and circularly polarized light beams interacting with cold atoms. *Phys Rev A* **79**(2), 023801-1–9 (2009)
57. Liao, J.Q., Law, C.K.: Parametric generation of quadrature squeezing of mirrors in cavity optomechanics. *Phys Rev A* **83**(3), 033820-1–4 (2011)

58. Truong, D.M., Nguyen, H.T.X., Nguyen, A.B.: Sum Squeezing, Difference Squeezing, Higher-Order Antibunching and Entanglement of Two-Mode Photon-Added Displaced Squeezed States. *Int J Theor Phys* **53**(3), 899–910 (2014)
59. Hofmann, H.F., Ono, T.: High-photon-number path entanglement in the interference of spontaneously down-converted photon pairs with coherent laser light. *Phys Rev A* **76**(3), 031806-1–4 (2007)

Publisher's Note Springer Nature remains neutral with regard to jurisdictional claims in published maps and institutional affiliations.

Springer Nature or its licensor (e.g. a society or other partner) holds exclusive rights to this article under a publishing agreement with the author(s) or other rightsholder(s); author self-archiving of the accepted manuscript version of this article is solely governed by the terms of such publishing agreement and applicable law.